DEVELOPMENT OF A COMPRESSION TEST FOR THICK COMPOSITE LAMINATES: FINITE ELEMENT ANALYSIS

Jasween Dogra*, J. M. Hodgkinson*, P. Robinson*, S. T. Pinho**
***The Composites Centre, Imperial College London, UK **Department of Aeronautics, Imperial College London, UK**

Keywords: *Thick laminate composites, compression testing, ICSTM fixture, specimen design, FEA*

Abstract

Finite element stress analyses have been made for composite laminates loaded in compression with a thickness of 2 mm and 10 mm, where the main parts of the fixture have also been modelled. Different designs have been investigated and the results are compared with a 2 mm thick specimen. Results for a reverse chamfer design and width waisted design for two different profiles are presented for a 10 mm thick specimen. A width waisted design has shown to significantly reduce stress concentrations in the fibre direction. A profile defined by a cubic equation offers the most promising results. The effect of including a model of the fixture grip in the transverse fibre direction on the specimen stress distribution is also considered for a 10 mm thick specimen. This has shown to increase the longitudinal stress concentrations in the specimen.

1 Introduction

A major concern in thick composite applications is undesired consequences associated with their apparent relatively low compression strength. Research has found that thick-section specimens can measure compression strengths up to 50% less than thin section specimens and failures are often not valid.

Existing fixtures which are capable of testing thick parallel-sided specimens include the IITRI [1], DTRC [2], NU [3], ICSTM [4] and Combined Load Compression (CLC) [5] fixtures. All use a combined shear and end loading method with the exception of the IITRI fixture which applied only shear load and the DTRC fixture which applies only end load to the specimen.

None of the fixtures mentioned are ideal. Investigations using the IITRI fixture report specimen buckling instability (Lamothe and Nunes [6]) and failure at the end tab termination region. The ICSTM and DTRC fixtures cause failure to occur in the end tab region of thick specimens instead of in the gauge section where stresses are uniform. The main disadvantage of the NU fixture is that the test procedure is not straightforward as ultimate timing of the end loading engagement depends on the specimen thickness. The Combined Load Compression fixture, which is a standard ASTM method [7], uses a multidirectional laminate design specimen. A back-out factor determines the strength of a UD ply but studies have shown that the 0° strength obtained depends on the angle ply orientation (Hoppel and Teresa [8], Lee and Soutis [9]).

Several studies investigate the use of a waisted gauge section design to promote failure in the gauge section, although few investigate thick waisted specimens. Shaw and Sims [10] tested 5 mm thick specimens circular waisted in 2D in the width direction. Similar results to parallel sided specimens were obtained but the stiffness properties were artificially increased by the non-uniform strain field produced as a result of waisting the specimen.

Anthoine et al [11] developed a new test configuration which uses a parallel sided specimen with through thickness tapered steel wedge grips bonded to the specimen using 1 mm thick adhesive as a substitute for end tabs. 2-D FE analysis showed stress concentrations in the fibre direction which normally develop at the end tab termination section in standard square end tabbed coupons were not present in the waisted steel wedge grip configuration.

This investigation is concerned with the cause of lower compression strengths in thick specimen and a new design in order to obtain the true compression strength of thick composites.

2. The ICSTM Compression Test Description

The ICSTM fixture [4] was chosen to develop a test for thick specimens. The ICSTM test procedure is straightforward to follow and uses a fixture which has a small volume of 1 m^3 and easy to replicate. The combined loading method involves shear loading the specimen via a torque applied to the inner and outer clamping screws in the fixture (refer to Fig 1). A torque of 5 Nm is applied to the inner bolt and 10 Nm is applied to the outer bolt; these specific torques were found to produce the optimum compression strength for 2 mm thick specimens. Shear load is transferred to the fixture through the clamping block and the specimen end tabs. End load is applied at a crosshead displacement rate of 1.0 mm s^{-1}.

The specimen uses a UD coupon design with reverse chamfered end tabs with a taper of 45˚. The gauge section length is 10 mm and the overall specimen length is 90 mm.

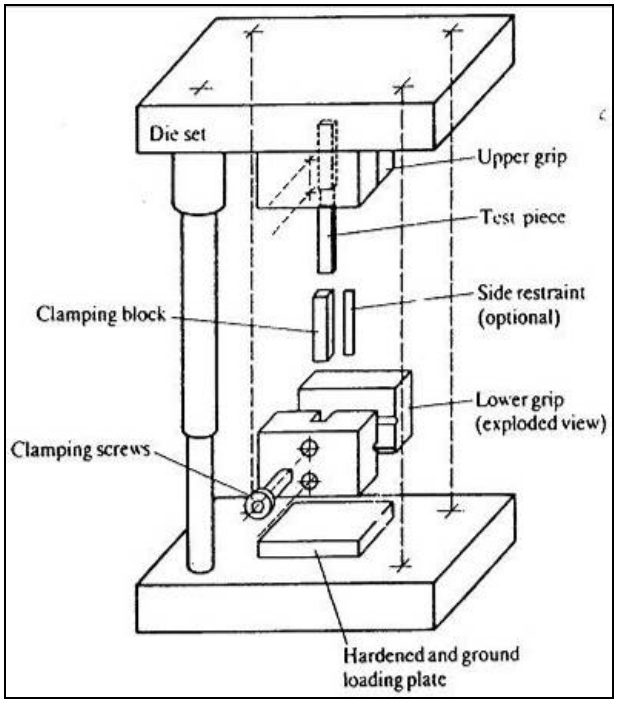

Fig 1. Schematic of ICSTM fixture [4]

3 Analysis Approach

3.1 Background

A computational approach was used in order to determine the effect of the specimen design on the stress distributions in the specimen. LSDYNA-3D explicit [12] was used to perform elastic dynamic analyses. Dynamic analyses allowed the full effect of preloading the specimen to be determined.

3.2 Finite Element Analysis Models

The sections of the fixture directly in contact with the specimen were included in the model analysis, as shown in Fig 2. The type of material used to model each part is shown in Table 1. The properties of these materials are presented in Table 2.

Table 1. Material types for different parts

Label	Part	Material type	Material
A	Carbon-fibre/epoxy composite	Orthotropic elastic	T300/914
B	End-tab	Orthotropic elastic	Woven EGlass/epoxy
C	Reverse chamfer epoxy	Elastic	3M Scotchweld adhesive
D	Clamping block	Elastic	Mild steel
E	Grip	Rigid	Mild steel
F,G	Inner,outer clamping bolt	Elastic	Mild steel

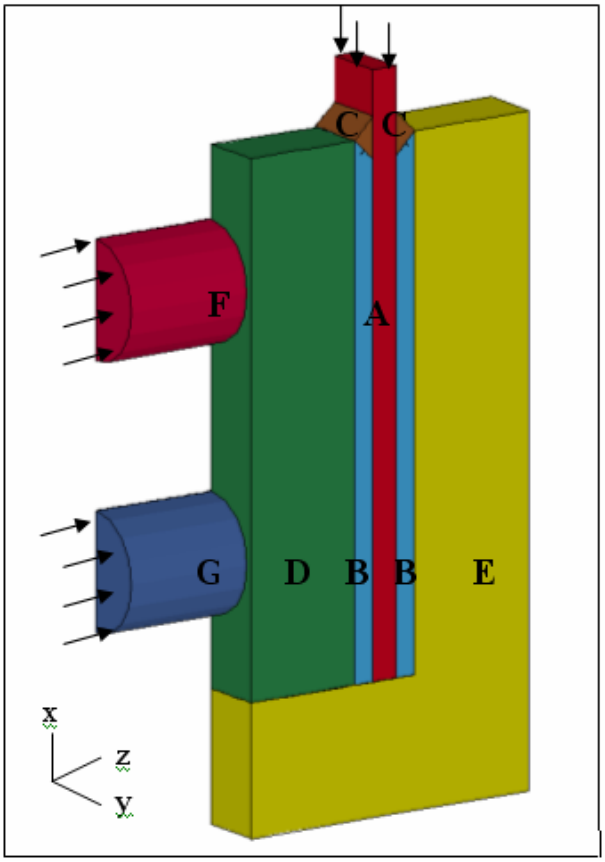

Fig 2. Reverse chamfer design model parts and loading conditions for 2 mm thick specimen

3.2 Finite Element Analysis Models

Each design modelled one quarter of the specimen since there are two planes of symmetry – transverse and longitudinal to the fibre direction. A comparison has been made of two different end tab designs - square end tab termination and reverse chamfer, both parallel sided (see Fig 4). The effect of specimen thickness on the stress distribution has been investigated for 2 mm and 10 mm thick specimens.

For the 10mm thick specimens, two different design profiles both with a width waisted gauge section have been analysed; these are defined by an elliptical and cubic function profile. The elliptical waisted profile is presented in Fig 4. No end tabs were included for the waisted profile designs. The waisted specimens were designed to have a minimum width of 6 mm at the gauge section in order to encourage failure at the ideal location.

Fixture models of two different complexities have been considered for the 10 mm thick specimen reverse chamfer design. In the complex case the fixture surrounds the specimen; in the simple case boundary conditions are used to represent the surrounding fixture. (see Fig 3).

The gauge length of each design is included in the figure; for the waisted design a 3 mm flat section at the centre allows the placement of a strain gauge. The end tab thickness is 1.6 mm in each case.

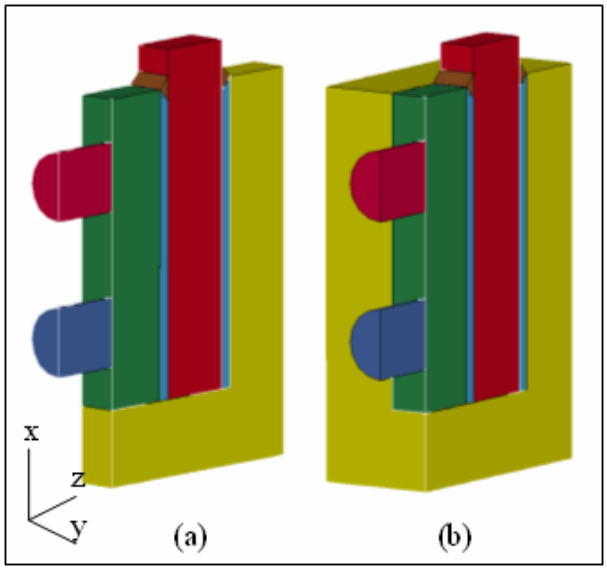

Fig 3. Model complexities: (a) simple model and (b) complex model for the 10 mm thick reverse chamfer design

A high mesh density was required in order to investigate the stress distributions in detail. Eight noded solid brick elements were used to model the specimen and all parts of the fixture. A minimum of 4800 elements were included in the carbon composite, depending on the specimen design, with the highest mesh density being in the end tab termination region. Sections of the meshes used for the different designs are presented in Fig 4. Alignment of the specimen in the fixture was assumed to be perfect.

Fig 4. Meshes for different specimen designs

(a) Square end tab design

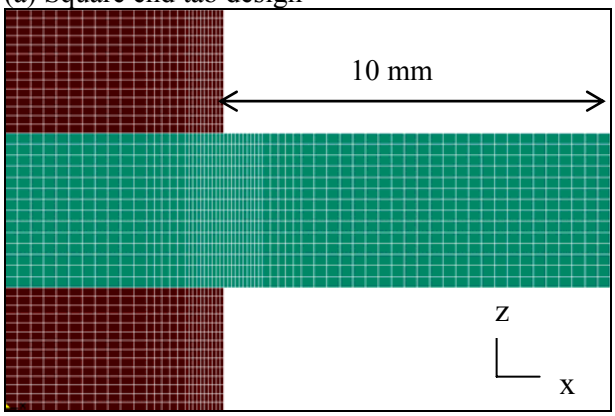

(b) Reverse chamfer design

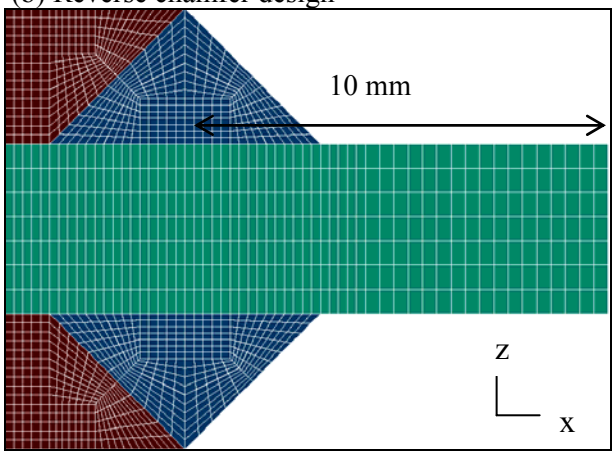

(c) Width waisted gauge section design for 10 mm thick specimen with an elliptical profile with a 6 mm width at the gauge cross-section

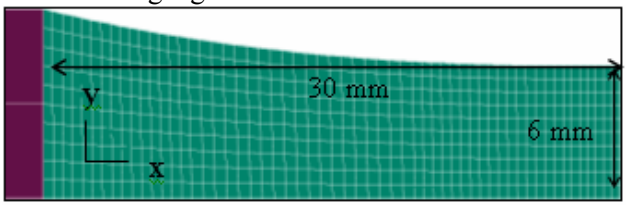

Table 2. Material properties

Material	E_{11}, GPa	E_{22}, GPa	E_{33}, GPa	G_{12}, GPa	G_{23}, GPa	G_{31}, GPa	υ_{21}	υ_{31}	υ_{32}
T300/914	129	8.4	8.4	4.2	3.0	4.2	0.02	0.02	0.40
Woven EGlass/epoxy	27	29	7	7.4	4.0	4.0	0.20	0.30	0.30
3M Scotchweld adhesive	2.87						0.37		
Mild steel	209						0.27		

The material system was UD T300/914 carbon epoxy, end tabs were woven cross-ply glass epoxy, the reverse chamfer design used an epoxy fillet, and the fixture was modelled in mild steel. The carbon-fibre/epoxy composite was assumed to have no imperfections. Properties for T300/914 were taken from [13]. The in-plane properties for the woven EGlass/epoxy were measured experimentally; the out-of-plane data was obtained from [14]. The adhesive properties were obtained directly from the manufacturer. Mild steel properties were obtained from [15].

3.3 Boundary Conditions and Loading Method

The boundary conditions are presented in Fig 5. The side face of the model was fully constrained in the y plane (transverse to the carbon fibre direction). The specimen gauge section was excluded in order to allow for Poisson's transverse expansion. The fixture grip was also fully constrained in the x and z planes (longitudinal and through-thickness relative to the carbon fibres).The degrees of freedom along the midline of the clamping screws were fully constrained in the x and y planes to prevent bending deformation.

The torque applied to the screws in the experiment was modelled as the equivalent uniform axial force. This was converted using equation (1) [16].

$$T = \mathrm{Pr}\tan(\alpha + \varphi) \quad (1)$$

T =Torque
P =Axial force
r = radius of bolt

$$\alpha = \tan^{-1}\left(\frac{np}{2\pi r}\right) \quad (2)$$

$$\varphi = \tan^{-1}\mu$$

n = Multiplicity of thread
p = Pitch
μ = Bolt material property

The axial force was applied as displacement directly to the bolts in the z direction. End loading of the specimen was applied as a uniform velocity directly to the carbon-fibre/epoxy specimen at the gauge cross section. This was applied in the x direction. The applied loads to the model are presented in Fig 2.

3.4 Model Contact Interfaces

For specimen models designed with end tabs, the nodes of the end tabs and carbon composite were merged together in order to represent the adhesive bond between them. Contact algorithms using a Coulomb friction coefficient of 0.3 were implemented between the specimen, the grip and the clamping block.

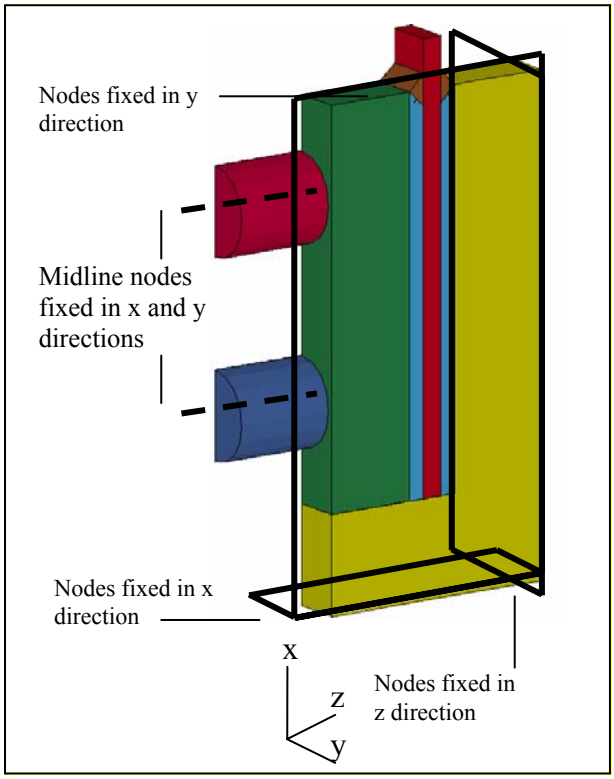

Fig 5. Model boundary conditions

4 Finite Element Analysis Results

The results presented correspond to a stress at the overall specimen mid-length cross section of 1500 MPa. This stress was a representative value of the compression strength of 2 mm thick reverse chamfer specimens, determined from experiments. The following data refers to elements at the composite mid-width along the surface closest to the clamping screws, as shown in Fig 6. The stresses did not vary significantly along the specimen width for parallel sided specimens. The stresses in the width waisted specimens showed variation in the width direction as shown in Fig 7, data was selected along the edge shown.

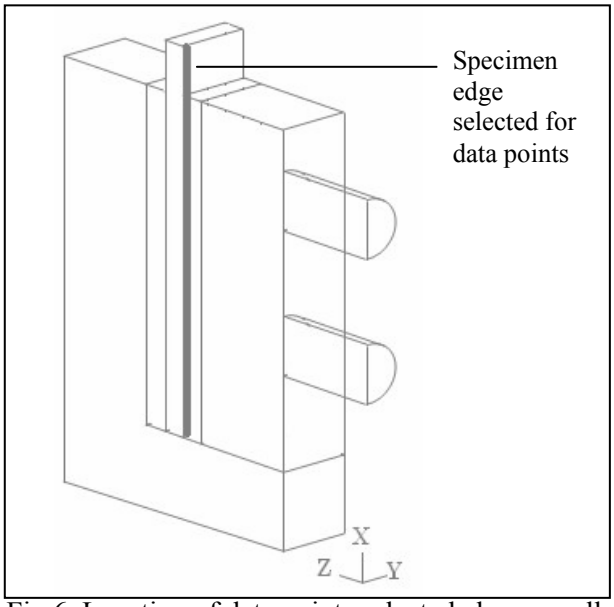

Fig 6. Location of data points selected along parallel sided specimens

Force balance equations in the longitudinal and through thickness directions were used to confirm overall equilibrium of the system. Values were input from the contact nodal forces between the part surfaces.

4.1 The effect of including a reverse chamfer

The effect of a reverse chamfer with a taper angle of 45° is presented. The predicted longitudinal stress distribution along the length of the specimen is shown in Fig 9. It confirms that the use of a reverse chamfer at the end tab termination region reduces the longitudinal stress concentration significantly. The stress gradient along the length of the specimen is due to the increase in shear stress contribution in the direction towards the gauge section.

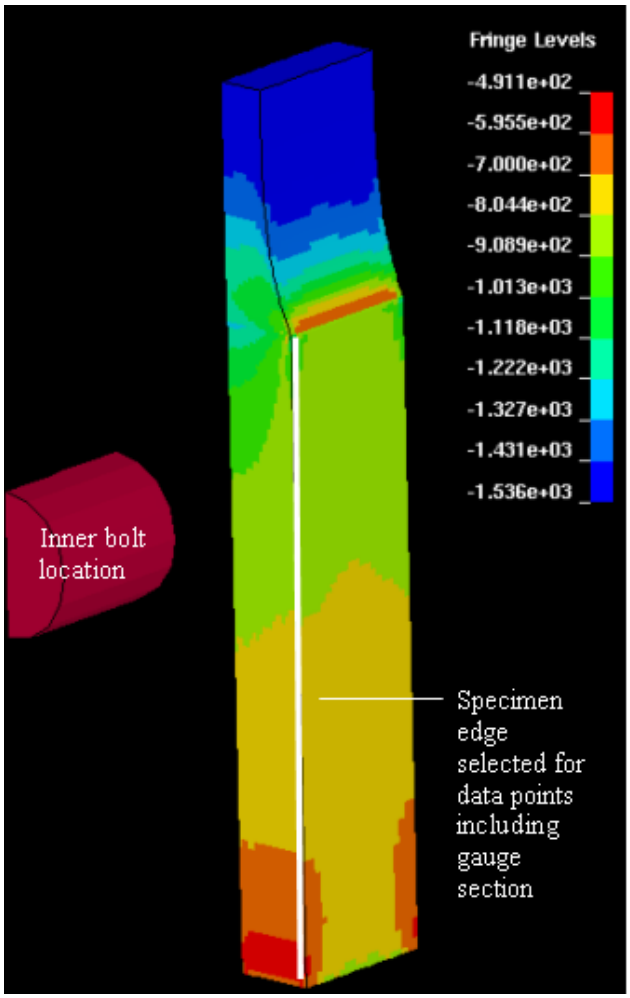

Fig 7. Predicted longitudinal stresses in width waisted specimen with a cubic function profile. The fringe levels show the stress values longitudinal stress values at failure time [MPa].

4.2 The effect of specimen thickness on stress distribution

The predicted longitudinal stress distribution along the length of the specimen for 2 mm and 10 mm thick reverse chamfer designs is shown in Fig 10. The stress gradient at the end tab termination region is significantly higher for the thicker specimen. This is due to potential greater expansion in both the through-thickness and transverse fibre directions for the thicker specimen. As a result this generates higher strains since the constraints are the same for both specimens so the specimen cannot expand. Table 3 shows the minimum and maximum transverse and through-thickness strains for the specimens confirming the presence of higher strains in the 10 mm thick specimen.

Table 3. Maximum and minimum transverse and through-thickness strains for 2 mm and 10 mm thick specimens

Specimen thickness [mm]		Strain	
		Transverse	Through-thickness
2	Min	-0.0067	-0.0049
	Max	0.0075	0.0082
10	Min	-0.0129	-0.0071
	Max	0.0080	0.0134

The node locations of these values were obtained. As expected, the maximum strains in both directions occurred at the end tab termination region on the carbon composite surface on the face closest to the clamping bolt. An example of this can be seen in Fig 8 for the 2 mm thick specimen. For the 10 mm thick specimen, the minimum through-thickness strain occurred on the same face of the carbon composite close to the end of the specimen, see Fig 8. This may represent end-crushing failure which often occurs during experiments. The minimum through-thickness strain is predicted to occur in the same location for the 10 mm thick reverse chamfer design, indicating that the use of end tabs may have little influence on end crushing failure.

Fig 8. Strain locations for the 2 mm and 10 mm thick specimen

(a) 2 mm thick specimen, location of maximum strain in the transverse direction in the gauge section. The fringe level shows the predicted strain values

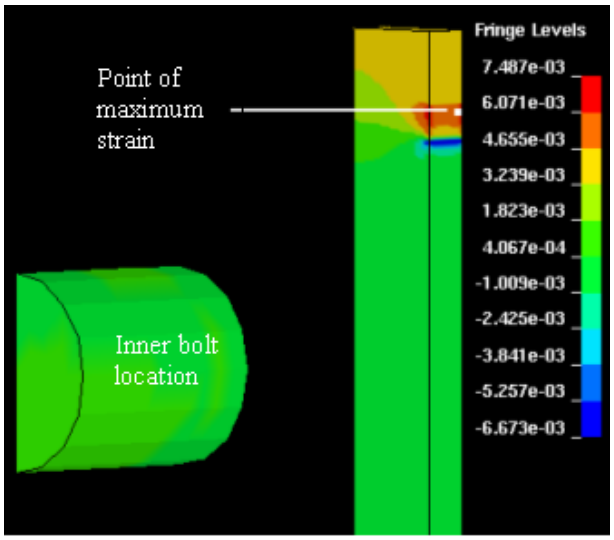

(b) 10 mm thick specimen, location of minimum strain in the through-thickness direction

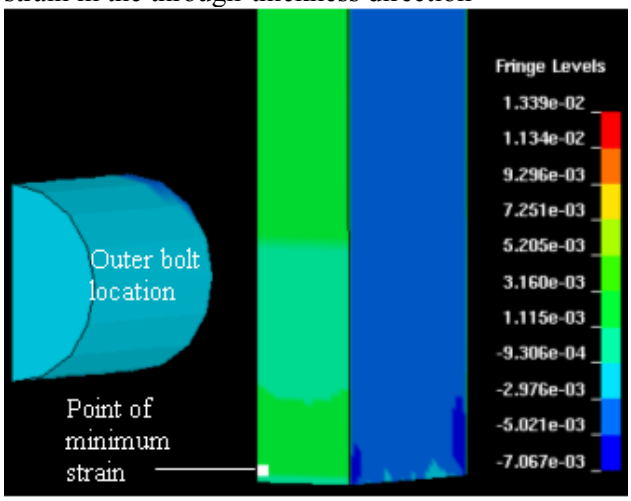

4.3 The effect of waisting thick specimens in the width direction

The predicted longitudinal stress distribution for width waisted specimens with different profiles is shown in Fig 11. The peak stress gradients for the waisted designs are significantly lower than for the reverse chamfer design. This is attributed to the more gradual change in geometry of the waisted specimens.

The use of a cubic function to determine the waisted profile gives a small improvement compared to the elliptical profile in the gauge length close to the flat section. This is due to the change in gradient where the waisted profile meets the flat section. For the cubic profile the second derivative at this location is zero, resulting in smaller longitudinal stress values compared to the elliptical profile

Fig 12 shows the through-thickness stress distribution along the specimen. The through-thickness stress gradients are significantly higher for waisted profile designs where the gauge section starts, due to the abrupt change in geometry. This may influence and change the compression failure mode, causing excessive matrix cracking and significant delamination compared to the reverse chamfer design.

Fig 13 shows the shear stress distribution along the specimen in the X-Y direction for waisted specimens and X-Z direction for the reverse chamfer design. Shear stresses in the X-Y direction for the reverse chamfer design were negligible. The shear stress gradients are significantly higher in the waisted profile designs at the start of the gauge section, attributed to the specimen geometry.

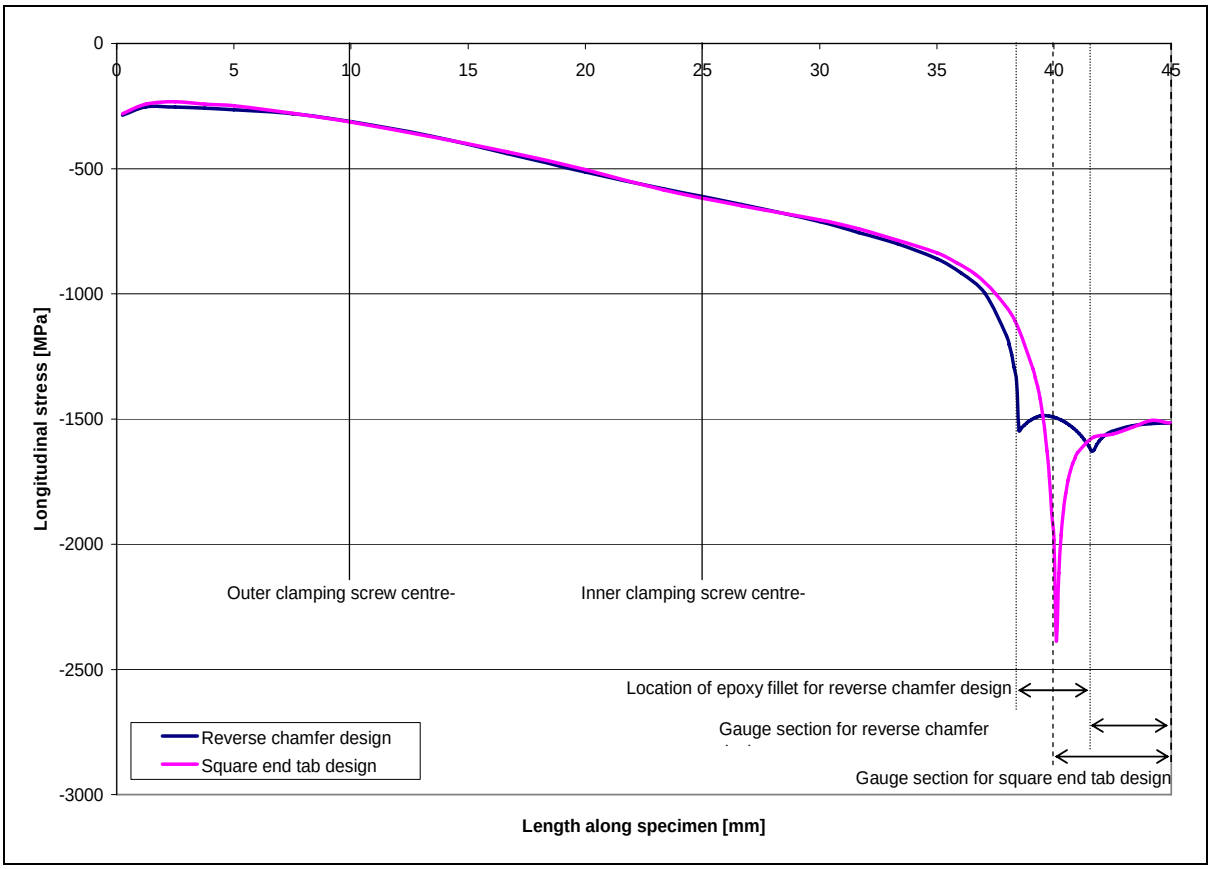

Fig 9. Longitudinal stress distribution along the length of the specimen for 2 mm thick specimen designs

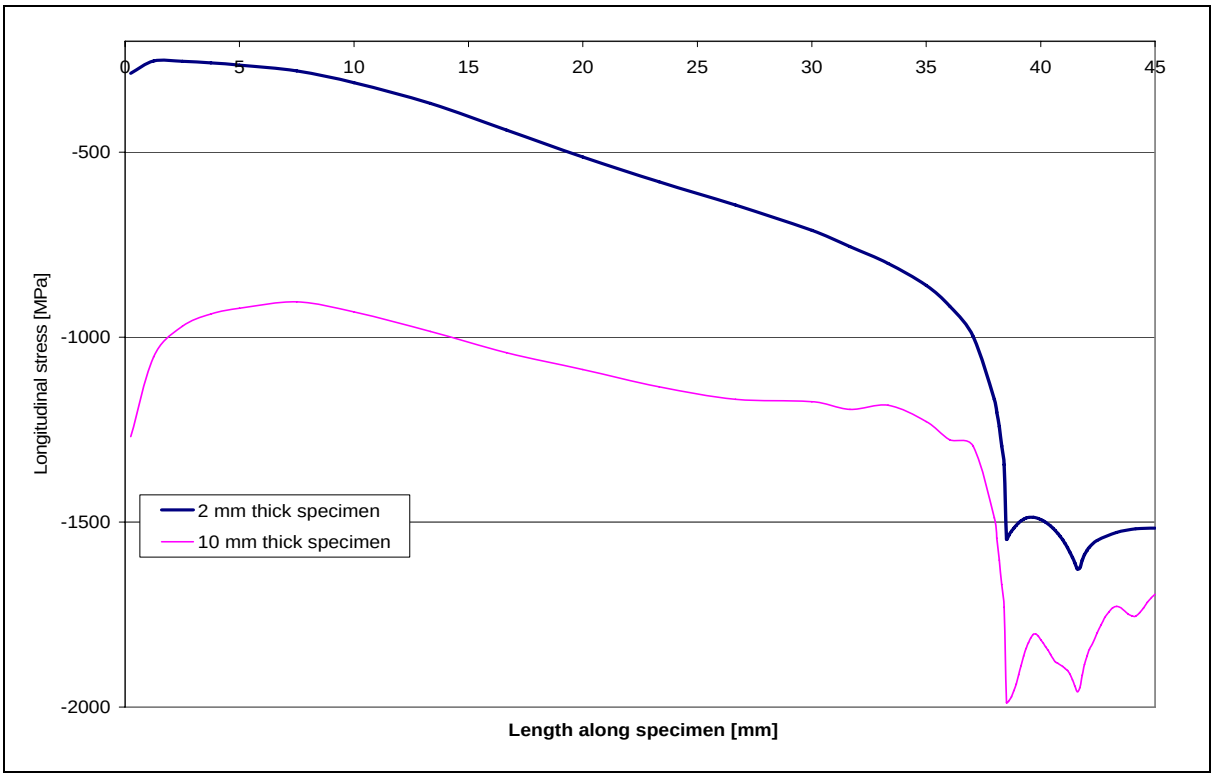

Fig 10. Longitudinal stress distribution along the length of the specimen for the reverse chamfer design for different specimen thicknesses

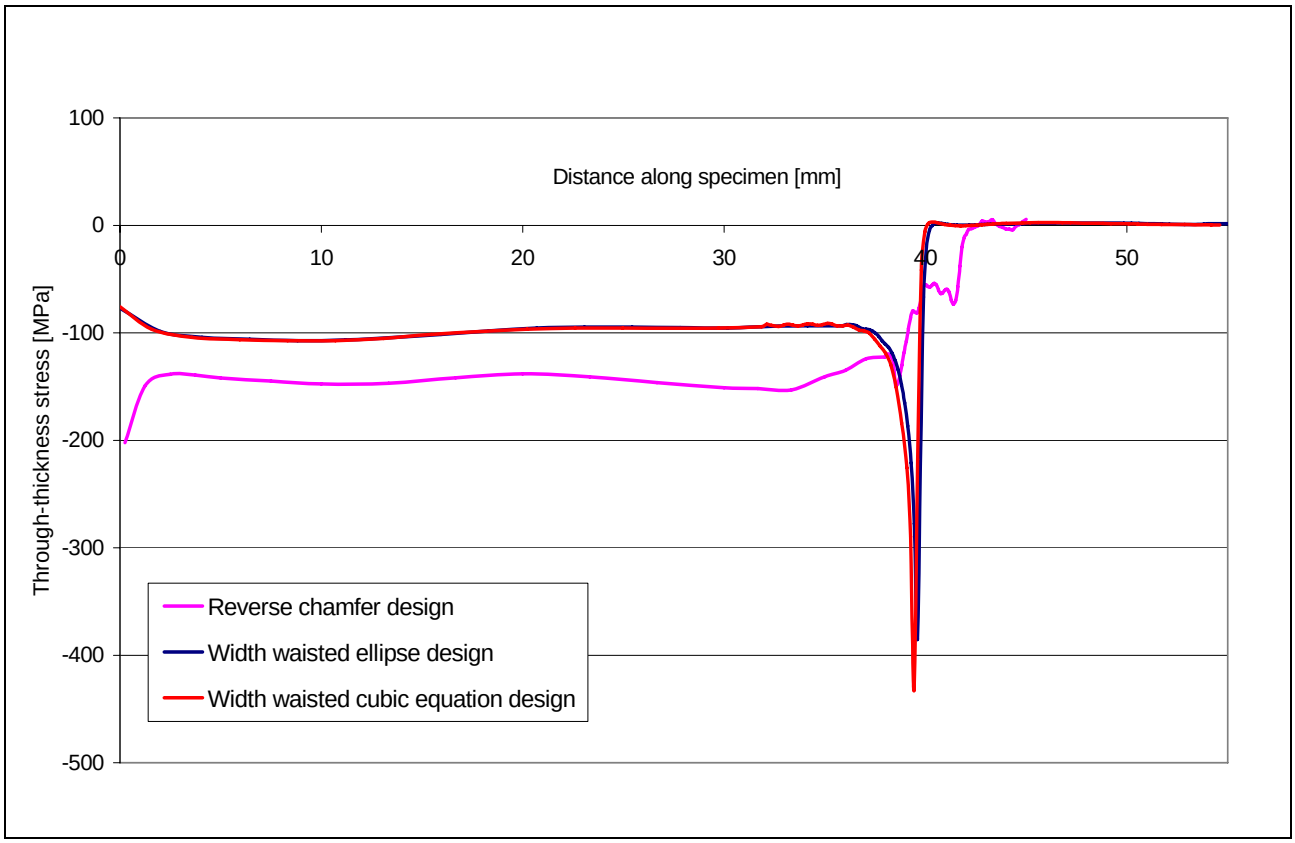

Fig 11. Longitudinal stress distribution along the length of the specimen for 10 mm thick specimen designs

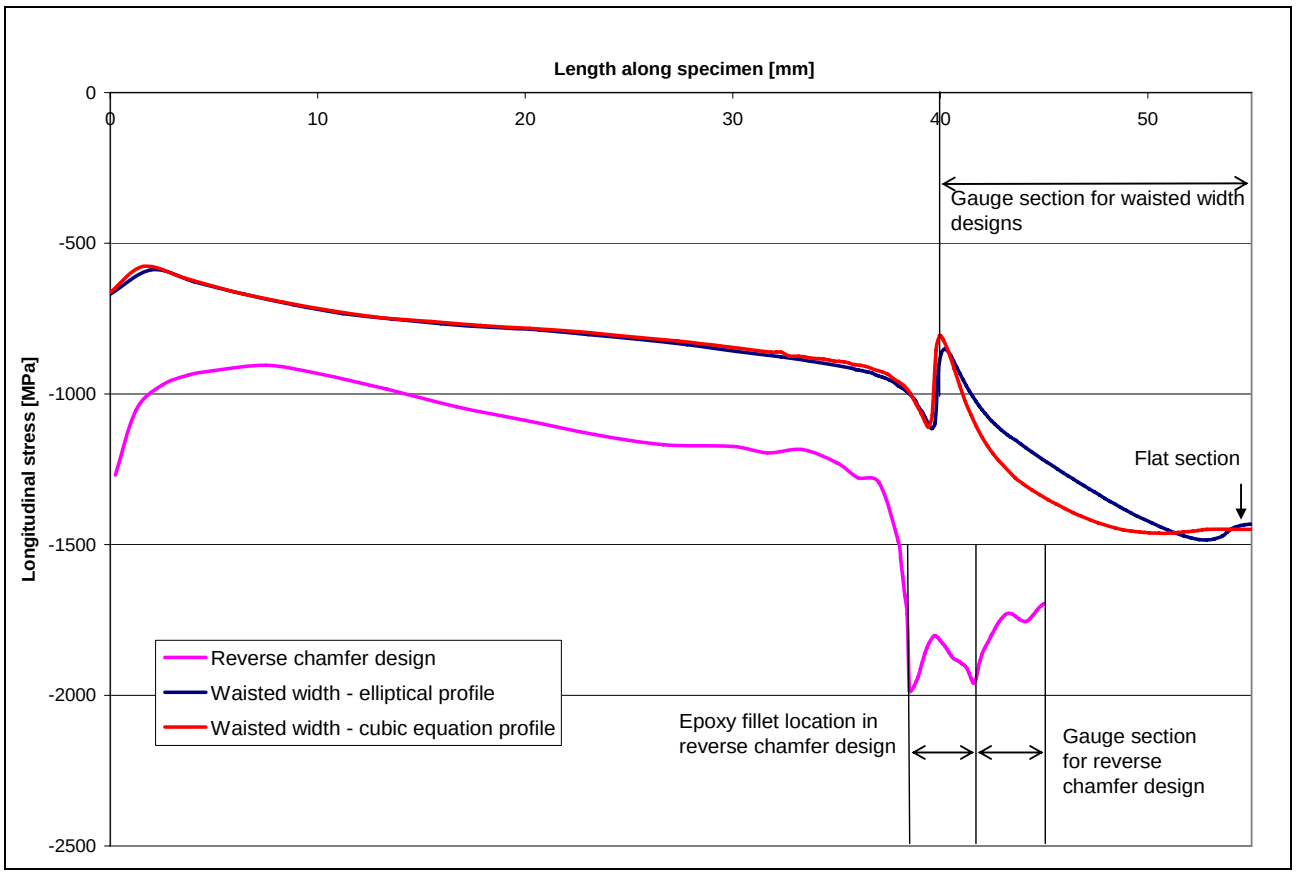

Fig 12. Through-thickness stress distribution along the specimen length for 10 mm thick specimen designs

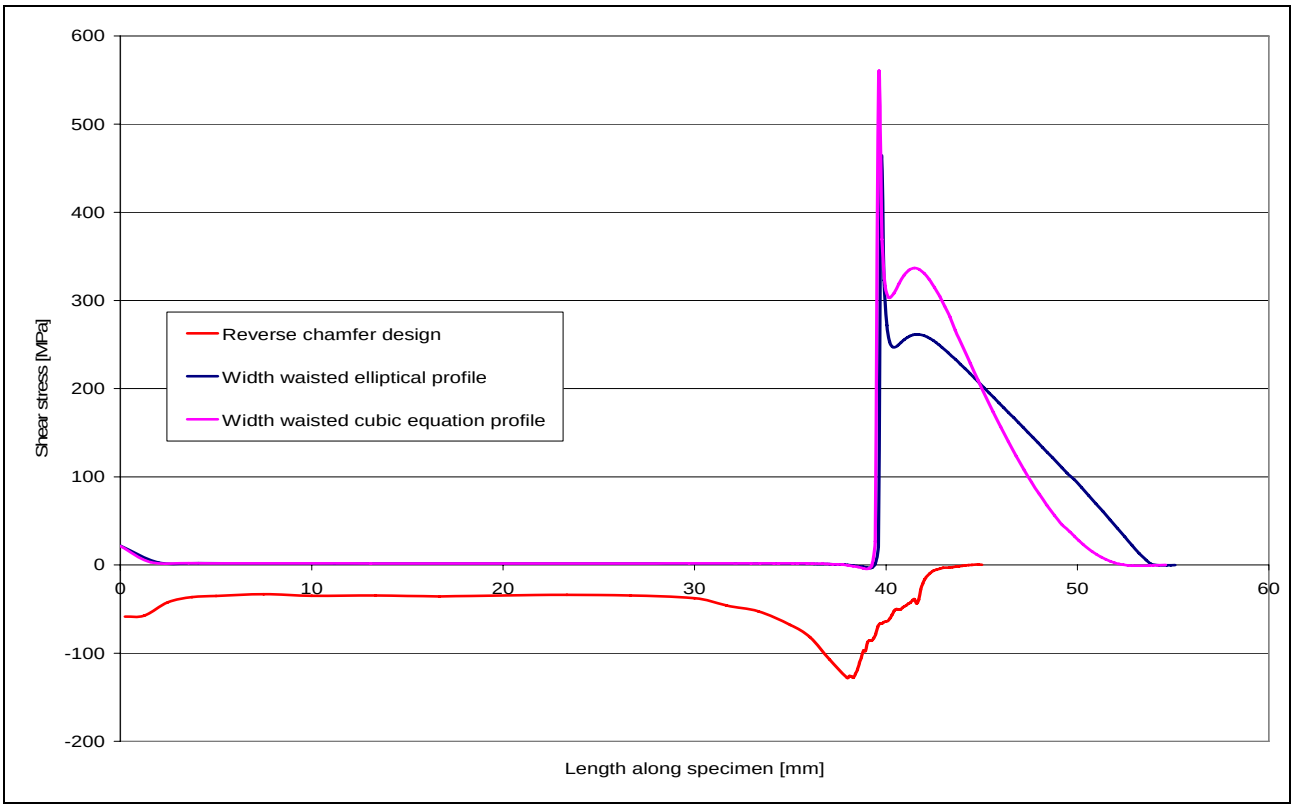

Fig 13.Shear stress distributions along the specimen length for 10 mm thick specimen designs

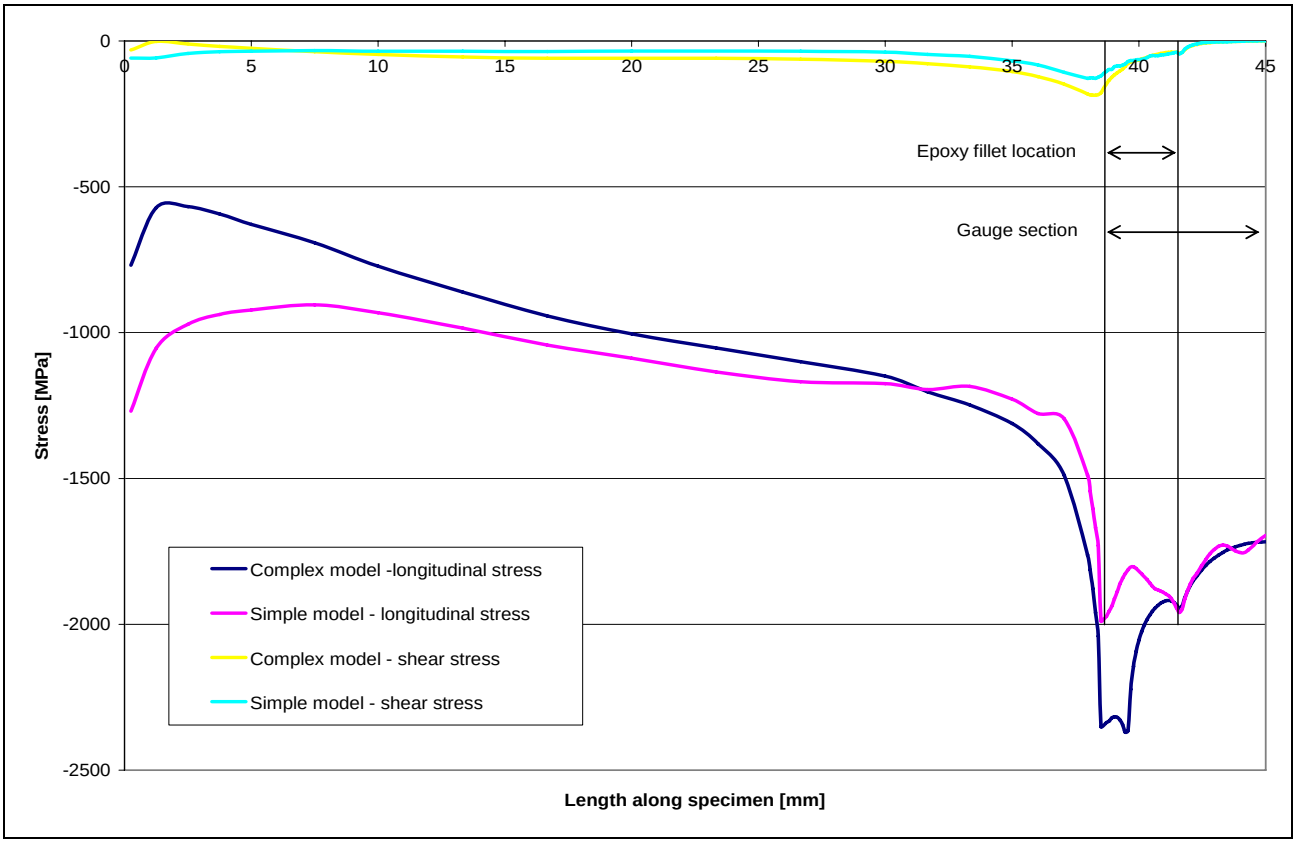

Fig 14. Longitudinal and shear stress distributions along the length of the specimen for different model complexities for a 10 mm thick reverse chamfer design specimen

4.4 The effect of using a more complex model

Fig 14 compares the longitudinal and shear stress distribution along the specimen length for two model complexities for the 10 mm thick reverse chamfer design specimen. The inclusion of the fixture in the fibre transverse direction results in a higher longitudinal stress gradient and higher peak stresses at the end tab reverse chamfer region. This is attributed to the higher shear stresses generated in the complex model due to the additional contact surfaces between the specimen and the fixture, confirmed by the shear stress distribution.

5 Conclusions

The results indicate that the fixture constraints in the fibre transverse and through-thickness directions may result in significantly higher stresses in thick compression specimens compared to thin specimens. The restricted expansion may also be the underlying cause of end-crushing failure observed when testing thick specimens.

Waisting thick specimens in the width direction offers one possible solution for reducing stress concentrations in the fibre direction. In particular, the use of a cubic function to define the profile has shown to be a potential solution. The use of a waisted profile causes higher through-thickness stresses and shear stresses at the start of the gauge section which may alter the failure mode.

Including the fixture model in the transverse specimen direction results in a higher longitudinal stress gradients at the end tab reverse chamfer region. This is attributed to higher shear stresses in the complex model.

Further work is required to optimise the waisted specimen design to reduce through-thickness and shear stress gradients for thick specimens. The effect of fixture on the specimen will be investigated further including the loading method and design of the gripping sections.

Some experimental work has already been done at Imperial College on 3-D circular waisted designs with 10 mm thick specimens waisted down to 6 mm at the centre [17]. Similar compression strength results to 2 mm thick specimens have been achieved. Further experiments are to be made.

6. References

[1] Rao P.N., Hofer K.E. "A new static compression fixture for advanced composite materials". *Journal of Testing and Evaluation*, Vol. 5, No. 1, pp 278-83, 1977.

[2] Camponeshci, E.T. *"Compression response of thick-section composite materials"*. University of Delaware, 1990.

[3] Daniel I.M., Wooh S.C., Hsiao H.M. "A new compression test method for thick composites*"*. *Journal of Composite Materials*, Vol. 27, pp 1789-806, 1995.

[4] Haeberle J.G. "Strength and failure mechanisms of unidirectional carbon fibre-reinforced plastics under axial compression". Imperial College London, 1992.

[5] ASTM D 6641/D 6641M "Standard test method for determining the compressive properties of polymer matrix composite laminates using a combined loading compression (CLC) test fixture". American Society for Testing and Materials, 2001.

[6] Lamothe R.M., Nunes, J. "Evaluation of fixturing for compression testing of metal matrix and polymer/epoxy composites". *Proceedings of Compression Testing of Homogeneous Materials and Composites*, Williamsburg USA, 1982.

[7] ASTM D 3410/D 3410M "Standard test method for compressive properties of polymer matrix composite materials with unsupported gage section by shear loading". American Society for Testing and Materials, 2001.

[8] Hoppel C.P., De Teresa S.J. "Effect of angle ply orientation on compression strength of composite laminates". Army Research Lab, Aberdeen Proving Ground, 1999.

[9] Soutis C., Lee J. "Thickness effect on the compressive strength of T800/924C carbon fibre-epoxy laminates". *Composites Part A*, Vol. 36, No. 2, pp 213-27, 2005.

[10] Shaw R.M., Sims G.D. "Understanding compression testing of thick polymer matrix composites". National Physical Laboratory, Report DEPC-MN 019, 2005.

[11] Anthoine O., Grandidier J.C., Daridon L. "Pure compression testing of advanced fibre composites". *Composites Science and Technology*, Vol. 58, pp 735-7400, 1997.

[12] LS-DYNA-3D, Livermore Software Technology Corporation, version 971.

[13] Mespoulet, S. "Through-thickness test methods for laminated composite materials". Imperial College London, 1998.

[14] Adams D.F., Xie M. "Effect of specimen tab configuration on compression testing of composite materials". *Journal of Composites Science Technology and Research*, Vol. 17, No. 2, pp 77-83, 1995.

[15] Laminate-Analysis-Program, anaglyph Ltd. Version 4.0

[16] Kreith F. "The CRC handbook of mechanical engineering" 1st edition, CRC Press.

[17] Cheung H. "Compression behaviour of thick composite laminates". Imperial College London, 2006.